Indian J. Phys. **81(11)**, 1215-1226 (2007)

Review

The effect of magnetic field on wavy roll instability

Pinaki Pal[1] and Krishna Kumar[2]*

[1]Kabi Sukanta Mahavidyalaya, P.O.- Angus, Dist. - Hooghly, Pin - 712 221 West Bengal, India
[2]Department of Physics and Meteorology, Indian Institute of Technology, Kharagpur-721 302, West Bengal, India

E-mail : kumar@phy.iitkgp.ernet.in

Abstract : We present a low-dimensional model to study the effect of uniform horizontal magnetic field on wavy instability. The model is derived for the thermal convection in very small Prandtl-number-fluid, that shows direct transition from stationary two-dimensional rolls to three-dimensional waves at the onset of secondary instability. The flow kinetic energy shows both random bursting with power-law histogram as well as periodic behavior depending on the wavenumber *q* of the wavy perturbations. The uniform magnetic field applied along the roll axis suppresses the random bursting and leads to time-periodic waves for very low but finite Prandtl-number-fluids. The secondary instability appears in the form of periodic waves for wavy perturbations with smaller wavenumbers. The magnetic field suppresses the periodic waves leading to stationary two-dimensional rolls. Lowering of Prandtl number requires higher values of the magnetic field for the same effect. The results of the model compare well with those obtained from the model for zero-Prandtl-number convection.

Keywords : Wavy instability, thermal convection

PACS Nos : 47.20.-k, 47.70.Ht, 47.65.-d

Plan of the Article

*Corresponding Author

1. Introduction

Many dissipative systems display the dynamics showing random bursts with power-law size distributions [1]. They include cellular automatons [2], vibrating granular materials [3], continuous models based on nonlinear diffusion and noise [4], Burridge-Knopoff spring-block models [5] with coupled relaxation oscillators, and thermal convection [6]. Recently, a simple low dimensional deterministic model [7] derived for zero-Prandl-number convection showed random bursting in flow kinetic energy without any externally prescribed threshold such as maximum slope in sand-pile models, a maximum static friction in Burridge-Knopoff models or a given threshold in cellular automatons. The bursting in this model is due to the interaction of stationary and oscillatory instabilities at the onset of convection. The application of horizontal magnetic field on the other hand is known to inhibit the oscillatory instability [8-11]. Therefore, the magnetic field is likely to affect interaction of stationary and oscillatory instabilities and therefore the phenomenon of random bursting of the flow energy.

We present in this paper a low-dimensional model for interaction of stationary and wavy instabilities in the presence of a uniform horizontal magnetic field along the roll axis, close to the onset of convection in very low Prandtl number fluids. The secondary instability appears in the form of three-dimensional (3D) wavy instability [12]. The flow kinetic energy shows random bursts with powerlaw histogram, if the wavy perturbations have wavenumber q equal to critical wavenumber k_c of the two-dimensional (2D) rolls. The uniform magnetic field applied along the roll axis suppresses the random bursting and leads to time-periodic waves. For perturbations with smaller wavenumbers ($q < 0.6 k_c$), the secondary instability appears in the form of periodic waves. The magnetic field suppresses the periodic waves and leads to stationary rolls. Lowering of Prandtl number requires higher values of the magnetic field. The results obtained from this model for very low-Prandtl-number fluids compare well with those obtained from the model for zero-Prandtl-number convection [12]. They are also in qualitative agreement with the results of direct numerical simulation [9] and experiments [8] for mercury.

2. Hydrodynamical equations

We consider a thin horizontal layer of electrically conducting fluid of thickness d, uniform kinematic viscosity v, thermal diffusivity k, magnetic diffusivity λ confined between two flat boundaries, and heated underneath in the presence of a uniform horizontal magnetic field B_0 in the direction of the rolls (assumed along y-direction). The dimensionless hydrodynamic equations in Boussinesq approximation then read as :

$$\partial_t\left(\nabla^2 v_3\right) = \nabla^4 v_3 + R\nabla_H^2\theta + Q\hat{e}_3.\left[\nabla\times\nabla\times\left\{\partial_y b + P_m(b.\nabla)b\right\}\right] - \hat{e}_3.\nabla\times\left[(\omega.\nabla)v - (v.\nabla)\omega\right], \quad (1)$$

$$\partial_t\omega_3 = \nabla^2\omega_3 + \left[(\omega.\nabla)v_3 - (v.\nabla)\omega_3\right] + Q\hat{e}_3.\left[\nabla\times\left\{\partial_y b + P_m(b.\nabla)b\right\}\right], \quad (2)$$

$$P_r\left[\partial_t\theta + (v.\nabla)\theta\right] = \nabla^2\theta + v_3, \quad (3)$$

$$P_m\left[\partial_t b + (v.\nabla)b - (b.\nabla)v\right] = \nabla^2 b + \partial_y v, \quad (4)$$

$$\nabla . v = \nabla . b = 0, \tag{5}$$

where $v(x,y,z,t) \equiv (v_1,v_2,v_3)$ is the velocity field, $b(x,y,z,t) \equiv (b_1,b_2,b_3)$ the induced magnetic field, $\theta(x,y,z,t)$ the deviation in temperature field from the steady conduction profile, and $\omega \equiv (\omega_1,\omega_2,\omega_3) = \nabla \times v$ the vorticity field in the fluid. The dimensionless number $R = \alpha(\Delta T)gd^3 / vk$ is the Rayleigh number, $P_r = \frac{v}{k}$ the thermal Prandtl number, $P_m = \frac{v}{\lambda}$ the magnetic Prandtl number, α the the isobaric thermal expansion coefficient of the fluid, g the acceleration due to gravity, and ΔT the temperature difference across the fluid layer. The unit vector $\hat{e}_3$ is directed vertically upward. The Chandrasekhar number $Q = \frac{B_0^2 d^2}{\rho_0 \lambda v}$ is the measure of magnetic field, where ρ_0 is the reference density of the fluid. For most of the metallic fluids (*e.g.*, mercury or molten sodium) the thermal Prandtl number is of the order of 10^{-2}, while the magnetic Prandtl number is of the order of $10^{-5} - 10^{-6}$. Therefore we set $P_m = 0$ in eqs. 1, 2 and 4 for the remaining part of this paper.

The realistic *(no-slip)* conditions on the bounding surfaces require all components of the velocity field to vanish there for all time. We assume idealized *free-slip* conditions on the horizontal components of the velocity field at the bounding plates as they simplify the calculations. *Free-slip* conditions imply $v_3 = \partial_{zz} v_3 = 0$ at $z = 0,1$. The flat surfaces are considered perfect thermal conductor, which means the temperature perturbation $\theta = 0$ on the plates $(z = 0,1)$. The vertical magnetic field must be continuous at the horizontal boundaries located at $z = 0,1$. We used the boundary conditions for electrically conducting boundaries derived by Chandrasekhar [13] (§42). The vertical component of the magnetic field and the horizontal components of the electric field vanish at the bounding surface. For *free-slip* velocity conditions, these conditions translate to $b_3 = 0$ and the electric currents in horizontal plane vanish. That is, $j_i = j_2 = 0$ at $z = 0, 1$. The electric current j is defined by $j = \mathrm{curl}\, \boldsymbol{b}$.

3. The model

We employ the standard Galerkin technique to construct a low-dimensional model for very low-Prandtl-number convection in the presence of horizontal magnetic field along 2D-roll axis (y-direction). As we are interested in the effect of magnetic field on random bursting and wavy instability, which appear in the model [7] for zero-Prandtl-number convection, we choose identical modes for the vorticity field and extend the model to consider very low but finite values of Prandtl number. We expand all the fields in Fourier series compatible with the *free-slip*, thermally and electrically conducting boundaries and periodic boundary conditions in horizontal plane. They are :

$$v_3 = W_{101}(t)\cos(k_c x)\sin(\pi z) + W_{111}(t)\sin(k_c x)\sin(qy)\sin(\pi z) + \ldots, \tag{6}$$

$$\begin{aligned}\omega_3 = {} & Z_{010}(t)\cos qy + Z_{012}(t)\cos(qy)\cos(2\pi z) + Z_{111}(t)\cos(k_c x)\cos(qy)\cos(\pi z) \\ & + Z_{210}(t)\cos(2k_c x)\cos(qy) + \ldots,\end{aligned} \tag{7}$$

$$\theta = \theta_{101}(t)\cos(k_c x)\sin(\pi z) + \theta_{002}(t)\sin(2\pi z) + \theta_{111}(t)\sin(k_c x)\sin(qy)\sin(\pi z) + \ldots \quad (8)$$

The magnetic field is easily derivable from eq. (4) for the case of $P_m = 0$. Projecting the above modes on the hydrodynamic equations (eq.1 - eq.3), we arrive at the following model.

$$\dot{\zeta}_i = P_r\left[-d_{ik}\zeta_k + (a_i W_2 + c_i\zeta_4)W_1\right], \quad (9)$$

$$\dot{\zeta}_4 = P_r\left[-d_4\zeta_4 + \frac{\pi}{4}(2\zeta_1 - \zeta_2 + 3\zeta_3)W_1\right], \quad (10)$$

$$\dot{W}_1 = P_r\left[-d_5 W_1 + r_1\theta_1 + (e_1\zeta_1 + e_2\zeta_2 + e_3\zeta_3)W_2\right] - P_r(f_1\zeta_1 + f_2\zeta_2 + f_3\zeta_3)\zeta_4, \quad (11)$$

$$\dot{W}_2 = P_r\left[-d_6 W_2 + r_2\theta_2\right] + P_r(g_1\zeta_1 + g_2\zeta_2 + g_3\zeta_3)W_1, \quad (12)$$

$$\dot{\theta}_1 = -d_7\theta_1 + W_1 + P_r(h_1\zeta_1 + h_2\zeta_2 + h_3\zeta_3)\theta_2 + P_r\pi W_1\theta_3, \quad (13)$$

$$\dot{\theta}_2 = -d_8\theta_2 + W_2 + P_r(s_1\zeta_1 + s_2\zeta_2 + s_3\zeta_3)\theta_1 + P_r\pi W_2\theta_3, \quad (14)$$

$$\dot{\theta}_3 = -d_9\theta_3 - \frac{\pi P_r}{4}\left[2W_1\theta_1 + W_2\theta_2\right], \quad (15)$$

where the indices i and k can take values 1, 2, 3. The variables are renamed as : $(\zeta_1,\zeta_2,\zeta_3,\zeta_4) = (Z_{010},Z_{210},Z_{012},Z_{111})$, $(W_1,W_2) = (W_{010},W_{111})$, $(\theta_1,\theta_2,\theta_2) = (\theta_{101},\theta_{111},\theta_{002})$. $r = R/R_c$ is the reduced Rayleigh number. $d_{ik} = 0$ when $i \neq k$ and

$$d_1 = d_{11} = q^2 + Q,\ d_2 = d_{22} = \left(4k_c^2 + q^2\right) + \frac{Qq^2}{4k_c^2 + q^2},\ d_3 \equiv d_{33} = q^2 + 4\pi^2 + \frac{Qq^2}{\left(q^2 + 4\pi^2\right)},$$

$$(a_1,a_2,a_3) = \frac{\pi^2 q^3}{4k_c + \left(k_c^2 + q^2\right)}(1,-1,-1),\ (c_1,c_2,c_3) = \frac{1}{4\left(k_c^2 + q^2\right)}\left(\pi q^2,\ \pi\left(4k_c^2 + 3q^2\right),-\pi q^2\right),$$

$$d_4 = \left(k_c^2 + q^2 + \pi^2\right) + \frac{Qq}{k_c^2 + q^2 + \pi^2},\ d_5 = \left(k_c^2 + \pi^2\right),\ d_6 = \left(k_c^2 + q^2 + \pi^2\right) - \frac{Qq^2}{k_c^2 + q^2 + \pi^2}$$

$$d_7 = \left(k_c^2 + \pi^2\right),\ d_8 = \left(k_c^2 + q^2 + \pi^2\right),\ d_9 = 4\pi^2,\ e_1 = \frac{k_c\left(k_c^4 + k_c^2 q^2 + \pi^2 k_c^2 - q^2\pi^2\right)}{2q\left(k_c^2 + q^2\right)\left(k_c^2 + \pi^2\right)}$$

$$e_2 = \frac{k_c q\left(3k_c^2\pi^2 + q^2\pi^2 - k_c^4 - k_c^2 q^2\right)}{4\left(k_c^2 + q^2\right)\left(4k_c^2 + q^2\right)\left(k_c^2 + \pi^2\right)},\ e_3 = \frac{e_2}{q^2},\ f_1 = \frac{\pi k_c^2}{\left(k_c^2 + q^2\right)\left(k_c^2 + \pi^2\right)},\ f_2 = \frac{-1}{2}$$

$$f_3 = \frac{\pi k_c^2 q^2}{2(k_c^2+q^2)(4k_c^2+q^2)(k_c^2+\pi^2)},\quad g_1 = -\frac{k_c}{q},\quad g_2 = -\frac{k_c(k_c^2+q^2-3\pi^2)}{2q(k_c^2+q^2+\pi^2)},\quad g_3 = \frac{q^2 g_2}{4k_c^2+q^2}$$

$$h_1 = \frac{k_c}{2q},\quad h_2 = \frac{-k_c}{-4q},\quad h_3 = -\frac{k_c q}{4(4k_c^2+q^2)},\quad r_1 = \frac{27k_c^2\pi^4}{4(k_c^2+\pi^2)}r,\quad r_2 = \frac{27\pi^4(k_c^2+q^2)}{4(k_c^2+q^2+\pi^2)},$$

$$s_1 = \frac{k_c}{q},\quad s_2 = \frac{k_c}{2q},\quad s_3 = \frac{k_c q}{2(2k_c^2+q^2)}$$

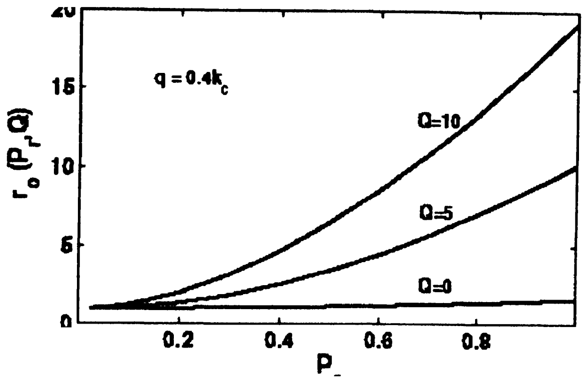

Figure 1. The threshold for secondary (wavy) instability as a function of Prandtl number P_r for different values of Chandrasekhar number Q. The wavy perturbations have a wavenumber $q = 0.4k_c$.

4. Results and discussions

First we switch off the magnetic field and integrate the model numerically using standard Runge-Kutta 4 method taking nondimensional time step equal to 0.005. We set critical Rayleigh number $R_c = 27\pi^4/4$ and the critical wavenumber $k_c = \pi/\sqrt{2}$, known values for 2D rolls [13]. The wavenumber q of periodic perturbations along the roll axis is also a parameter. We have studied the cases of $q = 0.4k_c$ and $q = k_c$ in detail. The integration is continued to make transients die away. Then, the magnetic field was switched on in small steps starting with a small value. Now we discuss the effect of uniform horizontal magnetic field along the axis of 2D rolls. For finite values of Prandtl number P_r, the convection always appears in the form of 2D stationary convection with freeslip thermally conducting horizontal boundaries [13] as the reduced Rayleigh number $r = R/R_c$ is raised above $r_c = 1$. In our model, the secondary instability appears as oscillatory instability, which leads to standing waves along the roll axis. This makes the convection three dimensional. We choose the wavy perturbations of wave number $q = 0.4k_c$. Figure 1 displays the effect of magnetic field on the critical value $r_o(P_r, Q)$ as a function of P_r for different values of Q. In the absence of magnetic field (Q=0),the onset

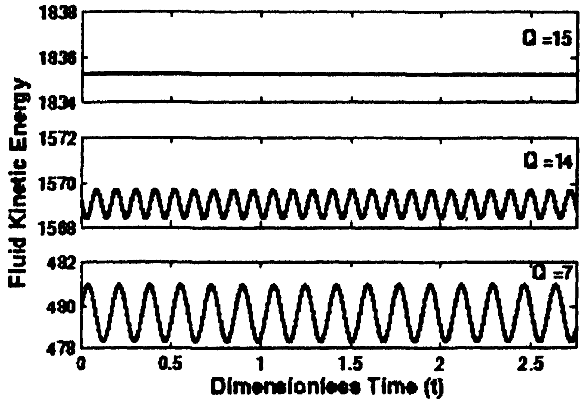

Figure 2. Fluid kinetic energy as a function of dimensionless time. Parameters are : $\epsilon = 5 \times 10^{-3}$, $P_r = 0.011$ and $q = 0.4\, k_c$.

value r_0, which is greater than r_c, increase slowly with increasing Prandtl number. In the presence of magnetic field $(Q \neq 0)$, the onset of the secondary instability is delayed. The horizontal magnetic field stabilizes 2D stationary rolls, which is known from simulations for thermal convection [14] with *no-slip* boundary conditions. We see the similar behavior for $q < 0.6k_c$.

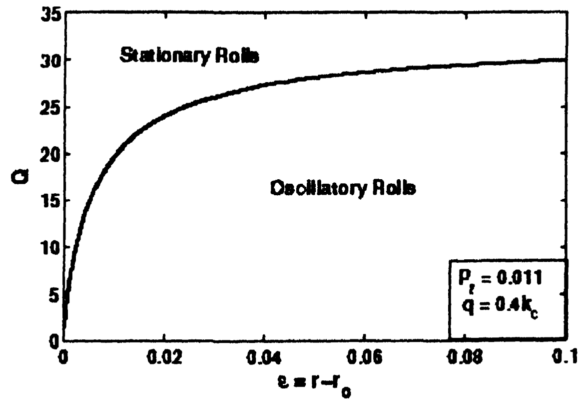

Figure 3. Stability boundary in the parameter space ϵ - Q. The wavy rolls are stable below the stability curve and two-dimensional rolls are stable above the curve. Parameters are : $P_r = 0.011$ and $q = 0.4\, k_c$.

If the time dependent oscillatory flow is subjected to uniform magnetic field, oscillatory convection is suppressed [15] in metallic fluids. We study this effect in our model by fixing reduced Rayleigh number $r = 1.005 > r_0 > r_c$ and then increasing the Chandrasekhar number Q in steps of unity. Figure 2 shows the flow kinetic energy of the oscillatory motion as a function of dimensionless time for three different values of Q for convective flow in molten sodium $(P_r = 0.011)$. If the magnetic field is above a value corresponding to Q=7, the amplitude

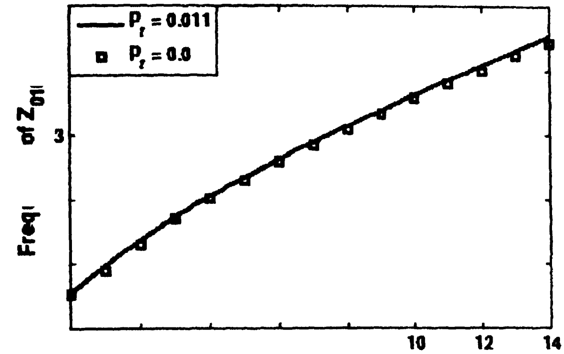

Figure 4. The frequency of Z_{010} as a function of Chandrasekhar number Q for two values of P_r. Other parameters are r = 1.005, q=0.4k_c.

of oscillation decreases and for Q = 15, the oscillation is completely suppressed. The frequency increases monotonically with increasing Q (see Figure 4). Figure 3 displays the stability boundary in the ϵ $-Q$ plane for molten sodium. Three-dimensional wavy rolls are stable for the parameters below the curve. Wavy oscillations are suppressed just above the curve, and stationary rolls appear.

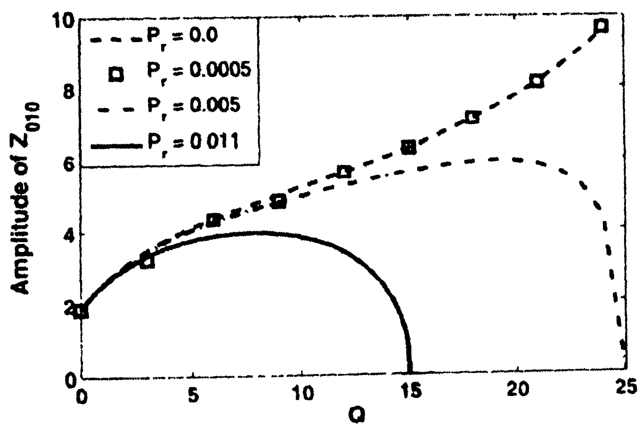

Figure 5. Oscillation amplitude of the mode Z_{010} as a function of Chandrasekhar number Q for various values of the Prandtl number P_r. The results for very small but finite value of P_r. agrees very well with those for P_r =0. Other parameters are r = 1.005, q=0.4k_c.

Figure 5 summarizes the effect of magnetic field on the amplitude of oscillation of the wavy roll mode Z_{010} at different values of the Prandtl number P_r for a fixed value of r close to its value for the wavy instability. It shows an interesting feature. The oscillation amplitude of wavy mode Z_{010} first increases with Q and then reaches a maximum before becoming zero. Since Figure 2 displayed the effect of raising Q starting from Q = 7, we observed oscillatory amplitude only

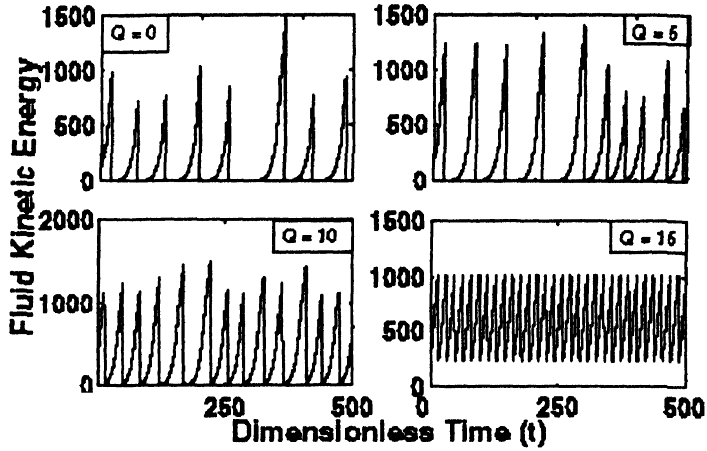

Figure 6. Time evolution of fluid kinetic energy at different values of Q. The parameters are : $\epsilon = 5\times10^{\ 3}$, $P_r = 0.011$ and $q = k_c$.

decreasing for sodium. As Prandtl number is decreased further, the suppression of wavy instability requires larger value of Q. For very low but finite values of $P_r (\leq 0.0005)$, the data agree very well with those obtained for the limiting case of $P_r \to 0$. This shows that the case $P_r \to 0$ is a smooth limit of our model. As growing 2D rolls are exact solutions [12] in the limit of zero P_r, we can never have stationary rolls. For any finite value of P_r, the stationary rolls appear for large Q. The frequency of the oscillation increases monotonically as observed in experiments [8].

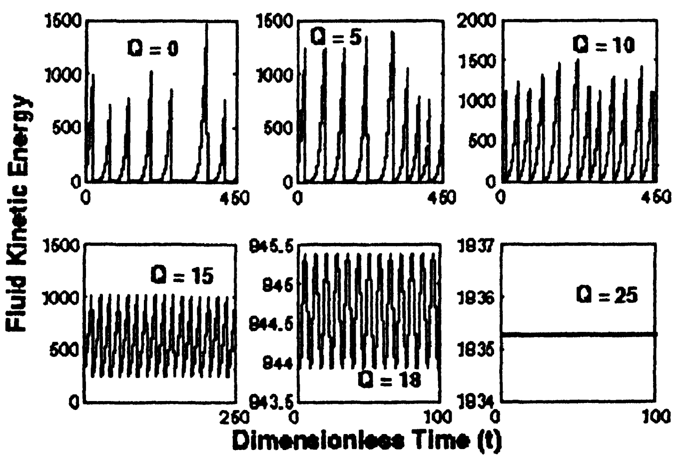

Figure 7. Time evolution of fluid kinetic energy at different values of Q. The parameters are : $\epsilon = 5\times10^{-3}$, $P_r = 0.011$ and $q = k_c$.

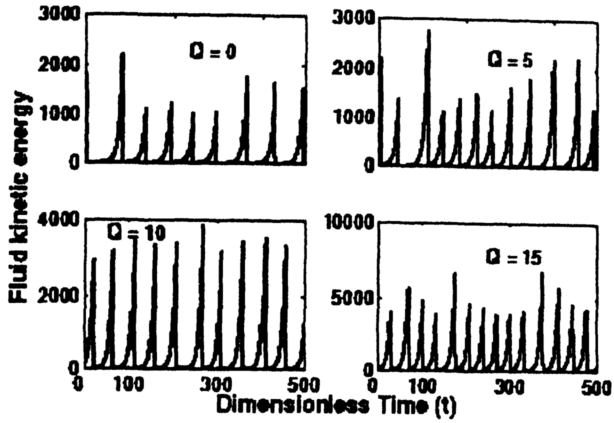

Figure 8. Fluid kinetic energy with time for various values Q. The parameters are : $\epsilon = 5\times10^{3}$, P_r = 0.0 and $q = k_c$.

Now we integrate the model (eqs. 9-15) for perturbative wavenumber $q = k_c = \pi/\sqrt{2}$. The convection sets in as 2D stationary rolls for r just above r_c in the case of finite value of P_r. For very low values of P_r, the wavy instability sets in close to the primary one. Figure 6 displays the fluid kinetic energy for various values of magnetic field. The wavy instability leads directly to chaos even in the absence of magnetic field. The flow energy shows nearly periodic or random bursts. The burst show a strong $t \rightarrow -t$ asymmetry. The time during which the roll energy increases is much larger than the time during which the energy is released. As the

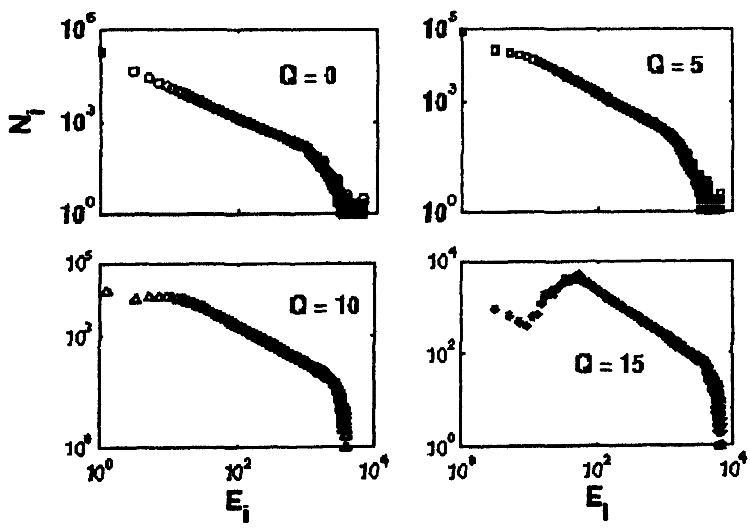

Figure 9. Fluid kinetic energy histogram at different values of Q. Parameters are same as in Figure 8.

magnetic field is switched on, the average time between two peaks decreases. Further raising Q leads to wavy solutions along the rolls. The magnetic field suppresses bursting in this case. For much higher value of Q (=25 for P_r = 0.011 and r = 1.005), the wavy motion of the rolls is also suppressed (see Figure 7) leading to stationary 2D rolls. As $P_r \to 0$ is approached, $r_0 \to r_c \equiv 1$, and stationary and oscillatory instabilities collide. In addition 2D rolls with saturated amplitude is no more a solution. So the application of magnetic field cannot lead to time-independent 2D rolls in this limit. The stationary instability make the amplitude of 2D rolls grow exponentially till wavy instability is triggered. It immediately dissipates the energy in very short time. Any fluctuations in energy due to various perturbations do not get time to decay out. This is the cause of randomness in flow energy bursts. As flow energy with bursts is the solution at the primary instability for $P_r \to 0$ case, we now study the effect of magnetic field on energy bursting in the limit $P_r \to 0$.

The zero-Prandt-number limit is obtained by setting $P_r = 0$ in the equations 1-4. The value of P_m remains set to zero as done in the previous case. The convective temperature field along with the perturbative magnetic field are now slaved. They can be determined from the velocity field and appropriate boundary conditions using eqs. 3-4. The model in this case becomes as :

$$\dot{\zeta}_i = -d_{ik}\zeta_k + (a_i W_2 + c_i \zeta_4) W_1 \tag{16}$$

$$\dot{\zeta}_4 = -d_4\zeta_4 + \frac{\pi}{2}(2\zeta_1 - \zeta_2 + 3\zeta_3) W_1 \tag{17}$$

$$\dot{W}_1 = -\tilde{d}_5 W_1 + (e_1\zeta_1 + e_2\zeta_2 + e_3\zeta_3) W_2 - (f_1\zeta_1 + f_2\zeta_2 + f_3\zeta_3)\zeta_4 \tag{18}$$

$$\dot{W}_2 = -\tilde{d}_6 W_2 + (g_1\zeta_1 + g_2\zeta_2 + g_3\zeta_3) W_1 \tag{19}$$

$\tilde{d}_5 = d_5 - \dfrac{27k_c^2\pi^4}{4(k_c^2+\pi^2)^2} r \quad \tilde{d}_6 = d_6 - \dfrac{27\pi^4(k_c^2+q^2)}{4(k_c^2+q^2+\pi^2)^2} r$, and other parameters are same as defined earlier. For Q =0, this system reduces to the model showing critical bursting [7].

We now present the results of the model (eqs. 16-19) for zero-prandtl-number convection in the presence of magnetic field. Figure 8 shows the effect of magnetic field on the fluid kinetic energy. The convection begins now just above r_c in the form of chaotic wavy rolls directly from conduction state. The amplitude of 2D rolls starts growing till a maximum value. Then rolls become wavy and roll energy is dissipated in a very short time. The process repeats itself. But the maximum value of the flow energy is different every time, and the time period between the energy peaks are not exactly equal. The bursts in flow energy are random. As Q is raised, the number of peaks as well as peak height increases. We now make sufficiently large number of energy bins with mean flow energy peaks are not exactly equal. The bursts in flow energy are random. As Q is raised, the number of peaks as well as height increases. We now make sufficiently large number of energy bins with mean flow energy E_i and small width ΔE_i and count the number N_i, the flow energy has acquired a value for i^{th} energy bin. Figure 9 displays the flow energy histogram for various values of Q on log-log scale. The power law remains intact for various values of Q. As Q increases, the distributions of flow energy peaks become narrow. This is consistent with the monotonic increase of frequency for oscillatory solutions for $q=0.4k_c$. The origin of power law here is structure of each burst and it does not result from averaging process of many bursts [7]. The flow energy signal consists of slow exponential growth followed by abrupt decrease to very small values. The flow energy signal consists of slow exponential growth followed by abrupt decrease to very small values. The probability $P(E)dE$ of finding flow energy between E and $E+dE$ is approximately proportional to time interval dt with $E \propto \exp(st)$. This leads to $P(E) \propto 1/E$. The magnetic field does effect the range of size distributions of flow energy peaks but not the power-law.

5. Conclusions

We have presented a low dimensional model to study the effect of horizontal magnetic field along the rolls on its dynamics. The mode shows the wavy instability of rolls may occur in the close vicinity of primary instability for very low-Prandtl-number fluids. Wavy instability with relatively longer wavelength leads to periodic oscillation. The horizontal magnetic field suppresses the oscillation and leads to stationary 2D rolls. The wavy instability with wavelength equal to the critical wave-length of the 2D rolls leas to random bursting of flow energy. The histogram of the flow energy with frequency shows power-law behavior. Stronger magnetic field suppresses the bursts in flow energy for low but finite values of Prandtl number. Zero-Prandtl-number convection shows random peaks in the flow energy even in the presence of relatively larger magnetic field with narrow size distributions. The probability distribution $P(E) \propto 1/E$ is fixed by each temporal structure rather than any averaging effect.

References

[1] P Bak, C Tan and K Wiesenfeld *Phys. Rev. Lett.* **59** 381 (1987); *Phys. Rev.* A **38** 364 (1988)

[2] D Dhar and R Ramaswamy *Phys. Rev. Lett* **63** 1659 (1989); D Dhar *Phys. Rev. Lett.* **64** 1613 (1990); K Wiesenfeld and J Theiler and B McNamara *Phys. Rev. Lett.* **65** 949 (1990); S S Manna *J Phys.* A **24** L 363 (1991); S Olami, H J S Feder and K Christensen *Phys. Rev. Lett.* **68** 1244 (1992); S Bottani *Phys. Rev. Lett.* **74** 4189 (1995)

[3] C Caponeri, S Douady, S Fauve and C laroche *Mobile particulate systems*, NATO ASI Series 287 (Kluwer) (eds) E Guazzelli and L Oger **19** (1995); J P Bouchaud, M E Cates, J Ravi Prakash and S F Edwards *J Phys.* I (France) **4** 1383 (1994); L Gill and D Sornette *Phys. Rev. Lett.* **76** 3991 (1996)

[4] G Grinstein and D H Lee *Phys. Rev. Lett.* **66** 177 (1991); T Hwa and M Kardar *Phys. Rev.* A **45** 7002 (1992)

[5] J M Carlson and J S Langer *Phys. Rev. Lett.* **62** 2632 (1989); M de Souza Vieira *Phys. Rev.* A **46** 6288 (1992)

[6] V Morin and E Dormy *Phys. Fluids* **16** 1603 (2004)

[7] K Kumar, P Pal and S Fauve, *Europhys. Lett.* **74** 1020 (2006); DOI:10.1209/epl/i2006-10051-7 (2006)

[8] S Fauve, C Laroche and A Libchaber *J. Phys. Letts. (France)* **42** L-455 (1981); *Ibid* **45** L-101 (1984)

[9] P Sulem, C Sulem and O Thual *Prog. Astro. Aeronaut.* **100** 125 (1985)

[10] A Juel, T Mullin, H Benhadid and D Henry *J. Fluid Mech.* **378** 97 (1999)

[11] B Hof, A Juel and T Mullin *J Fluid Mech.* **545** 193 (2005)

[12] O Thual *J. Fluid Mech.* **240** 229 (1992); K Kumar, S Fauve and O Thual *J. Phys. (France) II* **6** 945 (1996)

[13] S Chandrasekhar "*Hydrodynamic and Magnetohydrodynamic Stability*", *(Oxford : Oxford University Press)* (1961)

[14] F H Busse and R M Clever *J. Mech. Theo. Appl. (France)* **2** 495 (1983)

[15] M Meneguzzi, C Sulem, P L Sulem and O Thual *J. Fluid Mech.* **182** 169 (1987)